

TQD-Track: Temporal Query Denoising for 3D Multi-Object Tracking

Shuxiao Ding^{*,1,2} Yutong Yang^{*,1,3} Julian Wiederer¹ Markus Braun¹

Peizheng Li^{1,4} Juergen Gall^{2,5} Bin Yang³

¹Mercedes-Benz AG ²University of Bonn ³University of Stuttgart

⁴University of Tübingen ⁵Lamarr Institute for Machine Learning and Artificial Intelligence

{firstname.lastname}@mercedes-benz.com, gall@iai.uni-bonn.de, bin.yang@iss.uni-stuttgart.de

Abstract

Query denoising has become a standard training strategy for DETR-based detectors by addressing the slow convergence issue. Besides that, query denoising can be used to increase the diversity of training samples for modeling complex scenarios which is critical for Multi-Object Tracking (MOT), showing its potential in MOT application. Existing approaches integrate query denoising within the tracking-by-attention paradigm. However, as the denoising process only happens within the single frame, it cannot benefit the tracker to learn temporal-related information. In addition, the attention mask in query denoising prevents information exchange between denoising and object queries, limiting its potential in improving association using self-attention. To address these issues, we propose TQD-Track, which introduces Temporal Query Denoising (TQD) tailored for MOT, enabling denoising queries to carry temporal information and instance-specific feature representation. We introduce diverse noise types onto denoising queries that simulate real-world challenges in MOT. We analyze our proposed TQD for different tracking paradigms, and find out the paradigm with explicit learned data association module, e.g. tracking-by-detection or alternating detection and association, benefit from TQD by a larger margin. For these paradigms, we further design an association mask in the association module to ensure the consistent interaction between track and detection queries as during inference. Extensive experiments on the nuScenes dataset demonstrate that our approach consistently enhances different tracking methods by only changing the training process, especially the paradigms with explicit association module.

1. Introduction

3D Multi-Object Tracking (MOT) plays a crucial role in autonomous driving, embodied AI and mobile robotics. In re-

^{*}Equal contribution, names are sorted alphabetically.

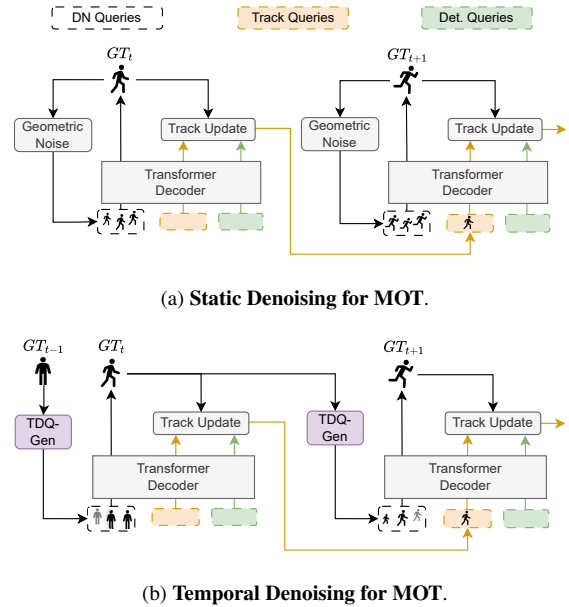


Figure 1. Comparison between static and temporal query denoising in MOT. Static denoising 1a generates denoising (DN) queries from the ground truths (GTs) of frame t by adding only geometric noise, tasking these DN queries to reconstruct the GTs at the same frame t . In contrast, our proposed temporal denoising 1b generates denoising queries from the GTs of the previous frame $t - 1$ using our novel temporal denoising query generator (TDQ-Gen) which considers various temporal-related noise types. These DN queries are then propagated to the current frame t , aiming to reconstruct their corresponding GTs at t instead of $t - 1$.

cent years, transformer-based 3D MOT methods [7, 8, 15, 23, 34] have gained significant attention due to their seamless integration into DETR-based detectors [4, 20, 28] or end-to-end autonomous driving systems [10]. Despite the promising performance, these methods struggle to deal with rare behaviors of other traffic participants or uncertain scenarios, e.g. in case of occlusion, limiting their robustness and scalability in real-world applications. Addressing this issue is essential for improving tracking reliability in highly

complex environments.

A common approach to increase the diversity of training samples is data augmentation, *e.g.* geometric transformations, or synthetic noise injection to simulate unexpected scenarios or model errors. However, too much noise in data augmentation could also lead to decreased training stability, leading to a trade-off between the diversity of simulated scenarios and performance boost.

Recently, there have been many attempts to explore denoising as an auxiliary training technique in the field of object detection, which has been proven to be effective. A prominent example is DN-DETR [13], which generates multiple groups of augmented queries from ground truths (GTs), adds noise onto them, and trains a DETR-like detector [4] to remove the noises and reconstruct GT boxes. Query denoising addresses the issue of slow convergence in DETR caused by inconsistent bipartite matching results during early training stages, where the denoising process decomposes the box refinement task from bipartite matching. Besides accelerating training, the augmented denoising queries allow introducing controlled perturbations, fulfilling the need of simulating diverse scenarios while not affecting the original training data. It enables modeling unexpected data or scenarios with higher noise level, demonstrating its potential for MOT to improve robustness against uncertainty.

However, the impact of denoising on 3D MOT remains unexplored. While recent studies [9, 37] investigate query denoising for MOT (Figure 1a), the process ignores temporal information, which is crucial for the MOT task. We refer to the conventional query denoising for MOT as *static query denoising* hereafter, as illustrated in Figure 1a. In addition, existing works [9, 37] build query denoising based on the tracking-by-attention paradigm, where data association is implicitly accomplished in the self-attention layer. However, query denoising requires a mask in self-attention to avoid that track and detection queries attend to the denoising queries, ensuring a consistent query interaction scheme as during inference. This limitation prevents the model to enhance data association through denoising queries. Consequently, effectively implementing query denoising in MOT remains a challenge.

To address the challenge, in this paper, we propose TQD-Track, which introduces Temporal Query Denoising that extends static query denoising to a streaming manner. As shown in Figure 1b, the denoising queries are generated by adding different types of noise to the ground truth detections of the previous frame $t - 1$ and then propagating them to the current frame t . The denoising queries are fed into the tracker as augmented inputs at current frame t and predict their corresponding ground truths box at timestep t . They emulate the track queries in a typical DETR-based tracker that carry temporal information and instance-specific fea-

ture representations, effectively enhancing the compatibility with MOT. Furthermore, we cover a wide range of uncertainty in training samples by ensembling various types of noise, including geometric noise, motion noise, query feature noise, and instance-level noise. We analyze the impact of temporal query denoising in three different transformer-based tracking paradigms, tracking-by-attention (TBA) [21, 32, 34], tracking-by-detection (TBD) [7], and alternating detection and association (ADA) [7]. The experimental results validate the conflict between implicit association using self-attention in TBA and the self-attention mask in query denoising, demonstrating the preference of query denoising in paradigms with explicit association module, *e.g.* TBD and ADA. For the explicit association module, we design an association mask with the same purpose as the self-attention mask in query denoising for object detection.

Extensive experiments on the nuScenes dataset [3] show that TQD-Track consistently improves the original trackers on all tracking paradigms and the superiority of temporal denoising over static denoising in 3D MOT. This validates our design to align query denoising with the MOT task. As our proposed method is a training strategy, the model architecture and the runtime during inference remain unchanged to the original tracker. The performance gain also shows the effectiveness of query denoising in increasing diversity of training samples to improve the robustness of the tracker.

2. Related Works

DETR-based Object Detection The advent of DETR [4] marked a paradigm shift in object detection by replacing hand-crafted components like anchor boxes and Non Maximum Suppression (NMS) with a transformer-based set prediction framework. Due to its flexibility, subsequent studies [5, 6, 13, 19, 22, 33, 38] have continuously introduced various optimized variants. For example, Deformable DETR [38] introduced deformable attention to enhance feature sampling efficiency, while Conditional DETR [22] accelerated convergence via conditional spatial queries. In 3D space, DETR3D [28] stands out as a seminal work, performing 3D object detection from multi-view images through a 3D-to-2D query projection based on Deformable Attention [38] using 3D reference points. PETR[20] enhanced spatial reasoning through position embedding transformation. Recent efforts [16–18, 26] leverage temporal information, achieving promising performance. These advancements demonstrate the adaptability of DETR in the handling both 2D and 3D detection, serving as foundation for downstream tasks such as multi-object tracking.

DETR-based Multi-Object Tracking TrackFormer [21] and MOTR [32] are pioneer works in conducting end-to-end Multi-Object Tracking based on DETR. They regard tracked objects as track queries that are propagated through

frames and aim to track the same object instances consistently, while object queries initialize new-born tracks. This establishes the tracking-by-attention (TBA) paradigm which has been further explored in 3D MOT [8, 10, 23, 34, 37]. However, recent works [7, 25, 31, 35] point out that TBA struggles in balancing both object detection and tracking tasks. Beyond TBA, DETR also enables end-to-end MOT with more traditional tracking-by-detection (TBD) paradigm, where objects are detected using DETR and then associated using heuristic [24, 30, 36] or learning-based methods [14, 15]. More recently, ADA-Track [7] proposes an alternating detection and association (ADA) paradigm, which integrates a learned data association module based on Edge-Augmented Cross-Attention [11] into each decoder layer and fully utilizes the synergy between detection and association. We build our temporal query denoising based on ADA-Track and show its potential in enhancing data association when learned data association module exists.

Query Denoising Vanilla DETR [4] faces the slow convergence issue because the Hungarian Matching provides inconsistent results to assign targets, resulting in instability in early training stage. DN-DETR [13] proposes the query denoising strategy, which effectively decouples the DETR training into a learning good anchors problem to better fit Hungarian Matching and a learning good relative offset problem for box regression tasks, leading to accelerated training and better performance. DINO [33] improves DN-DETR by adding negative samples in denoising queries. Query denoising has also become a standard training strategy in many 3D detection methods [20, 26]. Beyond object detection, SQD-MapNet [27] proposes a Stream Query Denoising (SQD) strategy that involves temporal modeling in the query denoising process for HD Map reconstruction task. DenoisingMOT [9] introduces query denoising into 2D MOT based on TBA, however, we found that TBA cannot fully benefit from query denoising for data association due to conflict between implicit association using self-attention in TBA and the masked self-attention in query denoising. To address this issue, we integrate denoising queries into the learned explicit association module from ADA-Track [7], leading to a denoising of data association task. We also include a Temporal Query Denoising inspired by [27] for temporal modeling. In doing so, query denoising is fully adapted for MOT task and contributes to modeling diverse unexpected scenarios in MOT.

3. Approach

The overview of the proposed TQD-Track is shown in Figure 2. As described in Sec 3.1, for a frame t , N_G groups of denoising queries are created from the ground truths of the previous frame $t - 1$ in the Temporal Denoising Query Generator (TDQ-Gen). Each denoising group combines various

types of noise, including geometric noise, query noise, motion noise, and instance-level noise. Together with track queries, the denoising queries are propagated from frame $t - 1$ to t . Following existing query denoising works, attention masks are applied to prevent leakage of ground truth information during training. As query denoising is a training strategy, the model architecture and inference process are identical to the original tracker, maintaining the same inference speed and model complexity. TQD-Track can be applied on several tracking paradigms, including *Tracking-by-attention* (TBA), *Tracking-by-detection* (TBD) and *Alternating Detection and Association* (ADA).

3.1. Temporal Query Denoising for MOT

Temporal Denoising Query Generator The Temporal Denoising Query Generator (TDQ-Gen) generates the denoising queries Q_{DN}^t during the transition phase between two subsequent frames, e.g. t to $t + 1$. TDQ-Gen takes as input the ground truth (GT) boxes B_{GT}^t , the track queries \hat{Q}_{T}^t , as well as the false positive detections $\{Q_{\text{FP}}^t, C_{\text{FP}}^t\}$, and outputs the denoising queries Q_{DN}^t and their corresponding 3D reference points C_{DN}^t :

$$Q_{\text{DN}}^t, C_{\text{DN}}^t = \text{TDQ-Gen} \left(B_{\text{GT}}^t, \hat{Q}_{\text{T}}^t, Q_{\text{FP}}^t, C_{\text{FP}}^t \right) \quad (1)$$

Each GT box $b_{\text{GT},i}^t = \{c_i, s_i, \theta_i, v_i\} \in B_{\text{GT}}^t$ is described by box center (also the reference point) $c_i \in \mathbb{R}^3$, box size $s_i \in \mathbb{R}^3$, yaw $\theta_i \in \mathbb{R}$, and the velocities $v_i \in \mathbb{R}^2$ in BEV plane. The denoising queries' bounding boxes B_{DN}^t are initialized from B_{GT}^t and inherit the instance IDs of corresponding GT boxes. For each denoising box $b_{\text{DN},i}^t$, the denoising query's features are copied from the track query of the same instance ID, i.e. $q_{\text{DN},i}^t = q_{\text{T},j}^t$ with $\text{ID}(b_{\text{DN},i}^t) = \text{ID}(q_{\text{T},j}^t)$. We then apply following types of noises on denoising queries:

1) **Center noise:** For the denoising reference point $c_{\text{DN},i}^t$ of i -th query, we first add uniform noise $(\Delta x_i, \Delta y_i, \Delta z_i)$ to the 3D GT box center c_i :

$$c_{\text{DN},i}^t \leftarrow c_{\text{DN},i}^t + [\Delta x_i, \Delta y_i, \Delta z_i]^T \quad (2)$$

A hyper-parameter λ is used to control the sampling range of noise which scales linearly to the object size $s = \{w, l, h\}$, i.e. $|\Delta x_i| < \frac{\lambda w}{2}$, $|\Delta y_i| < \frac{\lambda l}{2}$ and $|\Delta z_i| < \frac{\lambda h}{t}$.

2) **Query noise:** For the denoising query $q_{\text{DN},i}^t$, we add Gaussian noise onto the query feature $\epsilon_i^{\text{query}} \sim \mathcal{N}(\mathbf{0}, \Sigma^{\text{query}})$:

$$q_{\text{DN},i}^t \leftarrow q_{\text{DN},i}^t + \epsilon_i^{\text{query}}, \quad (3)$$

where $\epsilon_i^{\text{query}}$ has the same dimension as $q_{\text{DN},i}^t$. The purpose of adding Gaussian noise to the track query is to make the model more resilient to feature variations by using Gaussian noise to "blur" the feature representation.

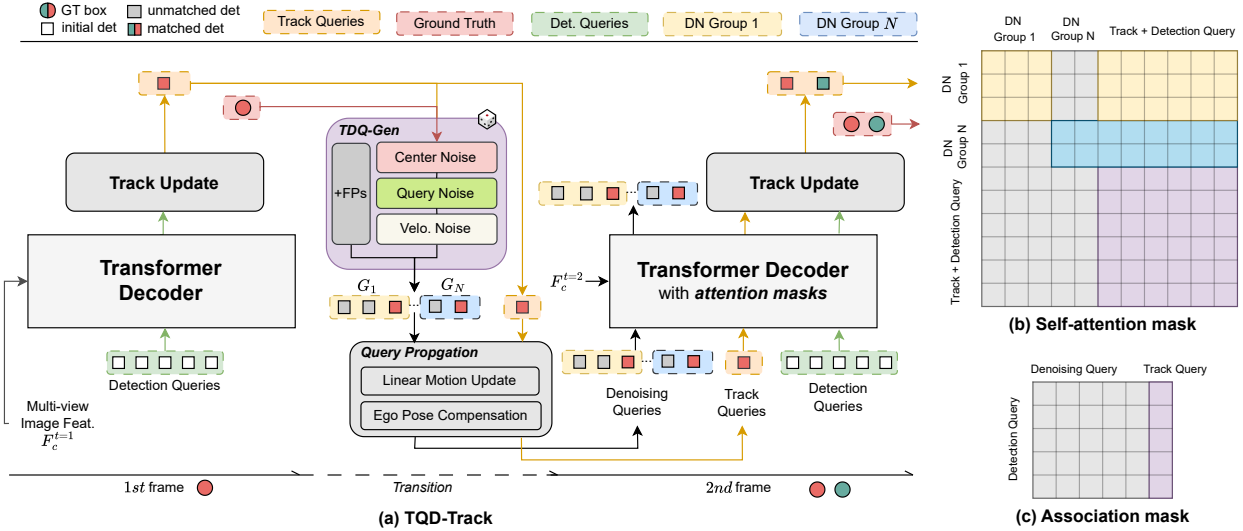


Figure 2. **Overview of TQD-Track applied on an DETR-based tracker.** For a frame $t - 1$, we generate several groups of denoising queries using the ground truth and add various noises onto them in the Temporal Denoising Query Generator (TDQ-Gen). The denoising queries are propagated to frame t , participate in the model as augmented input queries, and reconstruct their corresponding ground truth instance at the current frame t . Depending on the tracking paradigms, we use a self-attention mask (b) and/or an association mask (c) to align the forward pass during training with inference. Gray grids in (b) and (c) denote blocked attentions.

3) **Velocity noise:** Since the denoising queries will be propagated to next frame via a linear motion model, the velocities will play an important role in transition phase. Therefore we propose to also add Gaussian noise $\epsilon_i^{\text{velo}} \sim \mathcal{N}(\mathbf{0}, \Sigma^{\text{velo}})$ to the BEV velocities $v_{\text{DN},i}$:

$$v_{\text{DN},i} \leftarrow v_{\text{DN},i} + \epsilon_i^{\text{velo}} \quad (4)$$

The velocity noise simulates the uncertainty in the object’s motion, providing the tracker with more varied samples during training to enhance robustness.

4) **Instance-level noise:** Besides generating positive denoising queries which should be matched with GT boxes, Zhang et al. [33] introduce negative denoising queries which helps the model to respond to negative samples, *e.g.* predicting queries as background. In our temporal query denoising method, we achieve this by sampling false positive detections out of $\{Q_{\text{FP}}^t, C_{\text{FP}}^t\}$ as the negative denoising queries. Concretely, FP detections with top k confidence will be concatenated to the denoising queries, *i.e.*

$$Q_{\text{DN}}^t \leftarrow [Q_{\text{DN}}^t \parallel \text{TopK}(Q_{\text{FP}}^t)], \quad C_{\text{DN}}^t \leftarrow [C_{\text{DN}}^t \parallel \text{TopK}(C_{\text{FP}}^t)], \quad (5)$$

where $k = \alpha^{\text{FP}} N_{\text{GT}}^t$ with α^{FP} to control the ratio between number of negative samples (false positives) and GT instances. $[\cdot \parallel \cdot]$ denotes concatenation.

Denoising Groups We repeat the aforementioned process for N_G times to generate various denoising groups, producing a global set of denoising queries $\{Q_{\text{DN}}^{t,g}, C_{\text{DN}}^{t,g}\}_g$

where $g \in N_G$. The noise sampling for each denoising group g is independent to each other. In previous denoising works [13, 33], the types of added noise and the noise scales are constant across all denoising groups. We refer to this type of denoising groups as *general* denoising groups. In contrast, we introduce a novel approach to create denoising groups, termed *dedicated* denoising groups, where each denoising group is composed as a combination of dedicated noise types. In addition, *dedicated* denoising groups can also be combined with *general* denoising groups, resulting in *hybrid* denoising groups. The intuition behind *dedicated* and *hybrid* grouping is that we can train on specific noise types as well as on mixed noise types, leading to a better robustness against noise.

Query Propagation Once the denoising queries are generated using the aforementioned noising processes at $t - 1$, they will be propagated to the next frame t , same as the track queries. In addition, our proposed temporal query denoising also carries temporal information and instance-specific feature representations within denoising queries.

Denoising Process In standard static query denoising [13], denoising queries aim to reconstruct their corresponding ground truth boxes, regardless of timestamp. In contrast, in our proposed temporal query denoising, the denoising queries generated at the previous frame $t - 1$ and propagated to t reconstruct their corresponding ground-truth boxes at current frame t instead of these at $t - 1$. Hence,

the functionality of the denoising queries in our method is similar to the track queries in any DETR-based MOT method, as the track queries are tasked with detecting their corresponding ground truth instances at t that they have already detected at previous frame $t - 1$. This demonstrates that the design of our temporal query denoising is highly aligned with the DETR-based MOT, proven their compatibility from architecture level. The denoising queries are fed into the model as augmented track queries, participate into attending image features and interaction with detection queries together with the attention masks (*cf.* Section 3.2). The loss function related to denoising queries \mathcal{L}_{DN} is same as the loss for track queries. This results in the overall loss $\mathcal{L} = \lambda_{\text{DN}}\mathcal{L}_{\text{DN}} + \mathcal{L}_{\text{tracker}}$, where $\mathcal{L}_{\text{tracker}}$ is the loss of the basic tracker, depending on which method is used.

As a training strategy, the denoising queries are only generated during training, which ensures the same inference speed and model complexity as the baseline tracker.

3.2. Attention Masks

The attention mask is necessary in query denoising [13], ensuring consistent query interactions between detection and track queries as during inference. Depending on paradigms, different attention masks are used. TBA only requires masked self-attention, while TBD and ADA need additional mask for the data association module, *e.g.* masked edge-augmented cross-attention [11].

Self-attention mask In self-attention, we disable the detection and track queries to attend to the denoising queries while enabling attention in the opposite direction. Also, attentions between denoising queries in different groups are blocked, ensuring independency of each denoising group. Figure 2(b) illustrates the self-attention mask, where gray grid denotes the blocked attention. Formally, given $N_{\text{DN,all}} = \sum_g N_{\text{DN}}^g$ denoising queries, N_{T} track queries and N_{D} detection queries, where each individual denoising group $g \in G$ has N_{DN}^g queries, the self-attention mask can be denoted as $M_{\text{SA}} = [m_{ij}^{\text{SA}}]_{W \times W}$ where $W = N_{\text{DN,all}} + N_{\text{T}} + N_{\text{D}}$ is number of all queries and the queries are concatenated following the order: denoising queries, track queries, detection queries. The mask m_{ij}^{SA} between i -th and j -th query can be calculated as

$$m_{ij}^{\text{SA}} = \begin{cases} 1 & \text{if } j \leq N_{\text{DN,all}} \text{ and } \lfloor \frac{i}{N_{\text{DN},i}^*} \rfloor \neq \lfloor \frac{j}{N_{\text{DN},j}^*} \rfloor; \\ 1 & \text{if } j \leq N_{\text{DN,all}} \text{ and } i \geq N_{\text{DN,all}}; \\ 0 & \text{otherwise,} \end{cases} \quad (6)$$

where $N_{\text{DN},i}^* = \sum_g^{G_i} N_{\text{DN}}^g$ is the number of denoising queries that i can round down when accumulating denoising groups and $G_i^* = \max_G \left\{ \sum_g N_{\text{DN}}^g \mid \sum_g N_{\text{DN}}^g < i \right\}$ is the maximum possible group number.

Association mask When a learning-based data association module is employed, it updates the query features after interacting source and target queries, typically using cross-attention. In our method, denoising queries are viewed as augmented track queries, resulting in the unified query set $Q_{\text{U}} = \{Q_{\text{DN},1}, Q_{\text{DN},2}, \dots, Q_{\text{DN},N_{\text{G}}}, Q_{\text{T}}\}$. To align with the purpose of attention mask for query denoising methods, we need to prevent any feature flow from denoising query towards track or detection queries while keeping generating association-related features. To address this challenge, we propose an association mask which isolates query feature update from association feature, which is illustrated in Figure 2(c). Given unified denoising and track queries $Q_{\text{U}} \in \mathbb{R}^{(N_{\text{DN,all}} + N_{\text{T}}) \times d_k}$ as source and detection queries $Q_{\text{D}} \in \mathbb{R}^{N_{\text{D}} \times d_k}$ as target in cross-attention, the association mask $A_{\text{asso}} = \{m_{ij}^{\text{asso}}\}$ with $i \in [0, N_{\text{D}})$ and $j \in [0, N_{\text{DN,all}} + N_{\text{T}})$ can be formulated by

$$m_{ij}^{\text{asso}} = \begin{cases} 1 & \text{if } j < N_{\text{DN,all}}; \\ 0 & \text{otherwise.} \end{cases} \quad (7)$$

Given cross-attention a_{ij} between i -th query from Q_{U} and j -th query from Q_{D} , we can use the association mask m_{ij}^{asso} to calculate a masked softmax to normalize attention score solely among the track queries Q_{T} from Q_{U} , *i.e.*

$$\hat{a}_{\text{mask},ij} = \sigma_{\text{masked}}(a_{ij}) = \frac{(1 - m_{ij}^{\text{asso}}) \exp(a_{ij})}{\sum_k^{N_{\text{DN,all}} + N_{\text{T}}} (1 - m_{ik}^{\text{asso}}) \exp(a_{ik})}. \quad (8)$$

Using $\hat{A} = \{\hat{a}_{\text{mask},ij}\}$, we update detection queries by only aggregating track query features by $Q_{\text{D}} \leftarrow Q_{\text{D}} + \hat{A}(Q_{\text{T}}W_{\text{V}})$, where W_{V} denotes the learnable weights.

Different from query features, the features for association are established by each pair between Q_{U} and Q_{D} , corresponding to the edge features in a graph that connects nodes (queries). The association feature $E = \{e_{ij}\} \in \mathbb{R}^{(N_{\text{DN,all}} + N_{\text{T}})N_{\text{D}} \times d_k}$ between i -th source and j -th target nodes is generated by both node features $e_{ij} = f(q_i, q_j)$ or the attention $e_{ij} = f(a_{ij})$ or a combination of both where f denotes the learned association function. As the association features of each denoising-detection or track-detection pair are batched and stacked in a dimension, there is no information exchange between denoising-detection and track-detection pairs. Therefore, no masking is needed for association features, which enables learning data association between denoising and detection queries. To do so, the association feature is updated by the attentions A before masked softmax normalization, *i.e.* $E \leftarrow E + AW_{\text{E}}$.

4. Experiments

4.1. Experiment Setup

Dataset We conduct our experiments on the widely used nuScenes [3] dataset. The dataset comprises a total of 1,000

| Paradigm | Denoising Method | AMOTA \uparrow | AMOTP \downarrow | Recall \uparrow | MOTA \uparrow | IDS \downarrow | FP \downarrow | FN \downarrow | TP \uparrow | NDS \uparrow | mAP \uparrow |
|----------|--------------------|------------------|--------------------|-------------------|-----------------|------------------|-----------------|-----------------|---------------|----------------|----------------|
| TBA [34] | w/o Denoising | 0.443 | 1.299 | 0.552 | 0.416 | 175 | 11943 | 36861 | 64861 | 0.529 | 0.349 |
| | Static Denoising | 0.445 | 1.303 | 0.541 | 0.422 | 152 | 11561 | 37440 | 64305 | 0.539 | 0.350 |
| | Temporal Denoising | 0.446 | 1.280 | 0.561 | 0.432 | 175 | 12124 | 36221 | 65501 | 0.546 | 0.361 |
| TBD [7] | w/o Denoising | 0.483 | 1.249 | 0.603 | 0.451 | 797 | 13845 | 32640 | 68460 | 0.541 | 0.389 |
| | Static Denoising | 0.496 | 1.240 | 0.597 | 0.441 | 720 | 12668 | 33916 | 67261 | 0.538 | 0.391 |
| | Temporal Denoising | 0.503 | 1.229 | 0.602 | 0.458 | 708 | 13720 | 32228 | 68961 | 0.546 | 0.394 |
| ADA [7] | w/o Denoising | 0.493 | 1.208 | 0.602 | 0.450 | 672 | 14647 | 30422 | 70803 | 0.566 | 0.406 |
| | Static Denoising | 0.496 | 1.216 | 0.604 | 0.453 | 632 | 13588 | 31910 | 69355 | 0.559 | 0.404 |
| | Temporal Denoising | 0.515 | 1.206 | 0.623 | 0.467 | 596 | 13962 | 30460 | 70841 | 0.571 | 0.413 |

Table 1. Comparison of static denoising and temporal denoising methods on the nuScenes validation set for the Tracking-By-Attention (TBA), Tracking-By-Detection (TBD) and Alternating Detection and Association (ADA) tracking paradigms.

| Method | Backbone | Detector | AMOTA \uparrow | AMOTP \downarrow | Recall \uparrow | MOTA \uparrow | IDS \downarrow | FP \downarrow | FN \downarrow | TP \uparrow |
|------------------|----------|----------|------------------|--------------------|-------------------|-----------------|------------------|-----------------|-----------------|---------------|
| MUTR3D [34] | R101 | DETR3D | 0.294 | 1.498 | 0.427 | 0.267 | 3822 | – | – | – |
| DQTrack [15] | R101 | DETR3D | 0.367 | 1.351 | – | – | 1120 | – | – | – |
| STAR-Track [8] | R101 | DETR3D | 0.379 | 1.358 | 0.501 | 0.360 | 372 | – | – | – |
| MUTR3D* [34] | V2-99 | PETR | 0.443 | 1.299 | 0.552 | 0.416 | 175 | 11943 | 36861 | 64861 |
| DQTrack [15] | V2-99 | PETRv2 | 0.446 | 1.251 | – | – | 1193 | – | – | – |
| PF-Track [23] | V2-99 | PETR | 0.479 | 1.227 | 0.590 | 0.435 | 181 | – | – | – |
| ADA-Track [7] | V2-99 | PETR | 0.493 | 1.208 | 0.602 | 0.450 | 672 | 14647 | 30422 | 70803 |
| TQD-Track (Ours) | V2-99 | PETR | 0.515 | 1.206 | 0.623 | 0.467 | 596 | 13962 | 30460 | 70841 |

Table 2. Comparison of TQD-Track with existing methods on the nuScenes validation set. * denotes reproduced results.

| Method | AMOTA \uparrow | AMOTP \downarrow | Recall \uparrow | MOTA \uparrow | IDS \downarrow |
|------------------|------------------|--------------------|-------------------|-----------------|------------------|
| MUTR3D [34] | 0.270 | 1.494 | 0.411 | 0.245 | 6018 |
| PF-Track [23] | 0.434 | 1.252 | 0.538 | 0.378 | 249 |
| STAR-Track [8] | 0.439 | 1.256 | 0.562 | 0.406 | 607 |
| ADA-Track [7] | 0.456 | 1.237 | 0.559 | 0.406 | 834 |
| TQD-Track (Ours) | 0.511 | 1.154 | 0.592 | 0.461 | 625 |

Table 3. Comparison on nuScenes test set.

scenes, with 700, 150, and 150 scenes allocated for training, validation, and testing, respectively. Each scene spans 20 seconds and is annotated every 0.5 seconds, resulting in 40 keyframes per scene. The sensor set includes six surrounding cameras providing a 360° Field-of-View, along with LiDAR and radar. In our experiments, we use only multi-camera images as model inputs.

Evaluation Metrics We evaluate TQD-Track on the official primary MOT metrics of nuScenes, including Average Multi-Object Tracking Accuracy (AMOTA) and Average Multi-Object Tracking Precision (AMOTP) [29], as well as secondary metrics from CLEAR MOT [2], such as MOTA, MOTP, ID-switches (IDS), and Recall. In addition, we also report mean Average Precision (mAP) and the NuScenes Detection Score (NDS) to analyze the detection

performance. The detection metrics are averaged over the seven categories of the nuScenes tracking benchmark [3].

Implementation Details Following recent vision-only MOT works [7, 34], we use MUTR3D [34] as the Tracking-By-Attention (TBA) baseline and ADA-Track as the Alternating Detection and Association (ADA) baseline. Following [7], the Tracking-By-Detection (TBD) baseline is a PETR detector followed by the learnable data association layers based on [11]. All trackers are built based on PETR [34] with VoVNetV2 [12]. We strictly follow the training protocols of the corresponding baselines to ensure a fair comparison. The input images are cropped to 1600 × 640 and the tracker’s weights are initialized with a pre-trained PETR detector. Each training sample is a 1.5 seconds snippet with 3 consecutive frames, and the end-to-end tracker is trained for 24 epochs. All experiments are conducted on eight NVIDIA A100 GPUs with a batch size of 1 on each GPU. The hyper-parameters for denoising in TQD-Track are set as follows: The uniform center noise scale $\lambda = 1$; the velocity noise covariance $\Sigma^{velo} = \sigma_{velo} \mathbf{I} \in \mathbb{R}^{2 \times 2}$ where $\sigma_{velo} = 4$ and \mathbf{I} is the identity matrix; the query feature noise covariance $\Sigma^{query} = \sigma_{query} \mathbf{I} \in \mathbb{R}^{d_k \times d_k}$ where $\sigma_{query} = 0.1$ and $d_k = 256$; the false positive ratio $\alpha^{FP} = 0.1$; the number of denoising groups $N_G = 5$ generated by the hybrid grouping strategy.

We set the denoising loss weight λ_{DN} to 1 to balance the auxiliary denoising loss and the tracking loss.

4.2. Comparison of Query Denoising Methods

To demonstrate the generalization of TQD-Track across different DETR-based MOT paradigms, we compare our proposed Temporal Query Denoising with Static Query Denoising (Figure 1a) and the vanilla training strategy based on three paradigms: Tracking-By-Attention (TBA), Tracking-By-Detection (TBD), and Alternating Detection and Association (ADA). We include model details in the supplementary material and also refer to [7] for more details. All three baselines have the same backbone, detector, and the training settings as mentioned in section 4.1.

We show the comparison in Table 1. For TBA, both static denoising and our temporal denoising achieve similar performance and slightly outperform the AMOTA of the baseline w/o denoising, while our temporal denoising method significantly improves detection performance over the baseline without query denoising. As expected, TBA does not fully benefit from query denoising because of the conflict between the implicit association using self-attention in TBA and the masked self-attention in query denoising. On the other hand, for the paradigms with an explicit association module, *i.e.* TBD and ADA, our temporal denoising notably improves the MOT metrics over both baseline when query denoising is activated during training. This justifies our assumption that releasing the association task from the self-attention into a standalone module is much suitable for query denoising in MOT and validates the effectiveness of our design choice of integrating denoising queries into the data association module. Compared to TBA, query denoising contributes to more performance boost in MOT metrics than detection metrics, which further validates that properly applying query denoising in MOT contributes to a more balanced multi-task learning because MOT metric also takes detection performance into account. In addition our proposed Temporal Denoising further outperforms Static Denoising in both MOT and detection metrics, *e.g.* it leads to 4.5%pt increase in AMOTA and 11.3%pt less IDS compared to ADA-Track [7]. This demonstrates the effectiveness of incorporating temporal information into the denoising queries and enabling the model to remove temporal-related noises during training. Among all paradigms, TQD-Track with ADA-Track leads to a best performance, therefore, we use it as baseline in the following experiments.

4.3. State-of-the-art Comparison

Table 2 compares TQD-Track with existing transformer-based multi-camera 3D MOT methods on the nuScenes validation set. TQD-Track achieves the highest AMOTA and MOTA among all methods. Besides that, the higher AMOTA is also reflected in improved Recall. We attribute

the high Recall to the diverse noise types added in the temporal denoising queries, which simulates rare behaviors and model errors, improving the tracker’s robustness.

Furthermore, we report the performance of TQD-Track on the nuScenes test set in Table 3 and take the metrics of the baseline methods from the nuScenes leaderboard. For a fair comparison, we consider baselines that use the surrounding cameras as input and build on DETR3D or PETR detectors. TQD-Track outperforms the current leader, ADA-Track [7], by 5.5%pt in AMOTA and achieves 25% lower IDS, highlighting the effectiveness of our approach.

4.4. Ablation Study

We conduct ablation studies for the relevant parameters of our method. Ablation studies on denoising groups, denoising targets and denoising query composition are presented in the following. Additional ablation studies are discussed in the supplementary material.

Denoising Groups Table 4 shows the ablation study on the denoising group strategies, *General*, *Dedicated*, and *Hybrid*, and the number of denoising groups $N_G \in \{0, 1, 3, 5\}$. All denoising groups include instance-level noise in this ablation study. When only one *general* denoising group is applied, *i.e.* all noise types are used in this group, the tracking performance is similar to the baseline. This is outperformed by $N_G = 3$ denoising groups by 0.6%pt in AMOTA, showing the importance of multiple denoising groups to augment the training samples. With $N_G = 3$ denoising groups, we can use the *dedicated* grouping by injecting only one of the three noise types (center, velocity, and query noise) per group. This results in an 0.4%pt AMOTA increase compared to *general* grouping, highlighting the effectiveness of having *dedicated* noise groups to reduce interference between noise types. Interestingly, increasing the group number N_G from three to five doesn’t lead to an AMOTA increase for *general* grouping. By using our *hybrid* grouping strategy we can continue to improve the performance using more denoising groups. To form the *hybrid* group, we combine the three *dedicated* groups with two additional *general* groups. This configuration outperforms both, the model trained with $N_G = 3$ *dedicated* groups and the model with $N_G = 5$ *general* groups, by 1.2%pt and 1.7%pt AMOTA, respectively. It also achieves a notably higher Recall. This significant improvement underlines the benefit of *hybrid* grouping in leveraging the advantages of *general* and *dedicated* grouping strategies.

Consequently, we use 5 denoising groups with *hybrid* grouping as our default setting.

Denoising Targets We classify the noise types into three categories: the geometric noise, such as 3D center noise; the motion noise, including BEV velocity and query feature noise; and instance-level noise, such as the random ad-

| N_G | Strategy | AMOTA \uparrow | AMOTP \downarrow | Recall \uparrow | MOTA \uparrow | IDS \downarrow |
|-------|-----------|------------------|--------------------|-------------------|-----------------|------------------|
| 0 | – | 0.493 | 1.208 | 0.602 | 0.450 | 672 |
| 1 | General | 0.493 | 1.207 | 0.608 | 0.449 | 573 |
| 3 | General | 0.499 | 1.208 | 0.607 | 0.456 | 600 |
| | Dedicated | 0.503 | 1.202 | 0.614 | 0.461 | 592 |
| 5 | General | 0.498 | 1.197 | 0.606 | 0.446 | 643 |
| | Hybrid | 0.515 | 1.206 | 0.623 | 0.467 | 596 |

Table 4. Ablation study on the impact of the number of denoising groups N_G and the denoising group strategy.

| Exp. | Geometry | | | Motion | | Instance | | AMOTA \uparrow | AMOTP \downarrow | Recall \uparrow | MOTA \uparrow | IDS \downarrow |
|------|------------------------|------|-------|--------|-----|----------|--------------|------------------|--------------------|-------------------|-----------------|------------------|
| | Center | Velo | Query | Sample | FPs | | | | | | | |
| – | Baseline w/o denoising | | | | | | | 0.493 | 1.208 | 0.602 | 0.450 | 672 |
| 1 | | | | | | ✓ | 0.495 | 1.214 | 0.582 | 0.446 | 622 | |
| 2 | | ✓ | ✓ | | | ✓ | 0.505 | 1.205 | 0.591 | 0.456 | 614 | |
| 3 | ✓ | | | | | ✓ | 0.503 | 1.204 | 0.616 | 0.458 | 611 | |
| 4 | ✓ | ✓ | ✓ | | | | 0.495 | 1.223 | 0.602 | 0.452 | 610 | |
| 5 | ✓ | ✓ | ✓ | ✓ | | ✓ | 0.515 | 1.206 | 0.623 | 0.467 | 596 | |
| 6 | ✓ | ✓ | | ✓ | | ✓ | 0.498 | 1.198 | 0.606 | 0.458 | 624 | |
| 7 | ✓ | ✓ | ✓ | | | ✓ | 0.501 | 1.196 | 0.607 | 0.454 | 548 | |

Table 5. Ablation study on the combination of noise types.

| DN Query | Query Noise | AMOTA \uparrow | AMOTP \downarrow | Recall \uparrow | MOTA \uparrow | IDS \downarrow |
|------------------------|-------------|------------------|--------------------|-------------------|-----------------|------------------|
| Zero init. | ✗ | 0.500 | 1.21 | 0.627 | 0.454 | 627 |
| | ✓ | 0.491 | 1.20 | 0.608 | 0.445 | 609 |
| Init. from track query | ✗ | 0.501 | 1.196 | 0.607 | 0.454 | 548 |
| | ✓ | 0.515 | 1.206 | 0.623 | 0.467 | 596 |

Table 6. Ablation study on the denoising query composition.

dition of false positives. Table 5 compares the impact of different combinations of these noise categories. We use 5 *hybrid* denoising groups in this ablation study. However, when one of the noise types is deactivated, we remove the corresponding *dedicated* group while adding an additional *general* group to keep the total group number. When only considering the instance-level noise (Exp. 1) or only considering geometric and motion noises (Exp. 4), the model achieves similar tracking performance as the baseline, suggesting that a better combination of denoising targets is needed. Adding only geometric (Exp. 3) or motion (Exp. 2) noises on top of instance-level noises leads to a notably higher AMOTA. By adding all three categories together, the model achieves highest AMOTA of 0.515, outperforming the baseline by 2.2 %pt. This observation confirms our design choice of introducing the three different noise categories. In addition, when decoupling both noise types within motion noise (Exp. 6 and 7), the performance drops significantly. Here, the AMOTA decreases by 1.7 %pt and 1.4 %pt, respectively, compared to Exp. 5. And the AMOTA of Exp. 6 and 7 is even worse than Exp.

3 without any motion noise. This indicates that both, the velocity and the query feature representation, are closely related to each other by modeling changes in the object motion. This highlights the importance of introducing noise on both targets simultaneously.

Denoising Query Composition As shown in Eq. 3, the denoising query features are generated by adding Gaussian noise to the corresponding track query features. We justify our design choice by comparing with alternative choices of denoising query composition in Table 6. Specifically, we compare four DN query compositions: Query initialization as a zero vector with and without query noise as well as query initialization from the track queries with and without query noise. Without query noise, both DN query initializations achieve similar performance in all metrics except for IDS, where the initialization from track queries outperforms the zero initialization by 12.6 %. When query noise is added, the initialization from track queries shows a significant increase of 1.4 %pt in AMOTA compared to its noise-free counterpart, whereas the zero initialization method performs worse compared to its noise-free version indicated by a 0.9 %pt decrease in AMOTA. The higher improvements for the track query composition is that adding noises to the track queries can help the tracker to be more robust to uncertain query feature representations, where the Gaussian noise contributes to “blur” the objects’ appearance feature. Intuitively, the reason for the improvements for the track query initialization is that adding Gaussian noise can help the tracker to be more robust to uncertain object representations, like their appearances, which are encoded in the query features. In contrast, a zero initialized query vector does not contain any instance-specific information, such that adding noise only introduces confusion and reduces performance.

5. Conclusion

In this paper, we proposed TQD-Track, a query denoising method tailored for 3D Multi-Object Tracking (MOT), which augments training samples by injecting noises onto ground truth and enhances the ability to deal with uncertain scenarios. Targeting the temporal-specific nature of MOT, we introduced the temporal denoising method where denoising queries are generated in the past and propagated to the current frame, allowing awareness of temporal information and identity-consistent feature representations. We further investigated the impact of temporal denoising on three different tracking paradigms, tracking-by-attention, tracking-by-detection, and alternating detection and association, where we found that query denoising is most beneficial for the paradigms with an explicit association module. For these paradigms, we proposed the association mask alongside the existing self-attention mask in standard query denoising, which aligns query denoising with the model

architecture. TQD-Track outperforms the vanilla training method as well as the standard static query denoising on all paradigms while achieving state-of-the-art performance when applied on ADA-Track.

Acknowledgement

This work is a result of the joint research project STADT:up (Förderkennzeichen 19A22006O). The project is supported by the German Federal Ministry for Economic Affairs and Climate Action (BMWK), based on a decision of the German Bundestag. The author is solely responsible for the content of this publication.

The research leading to these results is funded by the German Federal Ministry for Economic Affairs and Climate Action within the project “NXT GEN AI METHODS – Generative Methoden für Perzeption, Prädiktion und Planung”. The authors would like to thank the consortium for the successful cooperation.

Juergen Gall has been supported by the Deutsche Forschungsgemeinschaft (DFG, German Research Foundation) GA 1927/5-2 (FOR 2535 Anticipating Human Behavior) and the ERC Consolidator Grant FORHUE (101044724).

References

- [1] Jimmy Ba, Jamie Ryan Kiros, and Geoffrey E. Hinton. Layer normalization. *ArXiv*, abs/1607.06450, 2016. [12](#)
- [2] Keni Bernardin and Rainer Stiefelhagen. Evaluating multiple object tracking performance: the clear mot metrics. *EURASIP Journal on Image and Video Processing*, 2008:1–10, 2008. [6](#)
- [3] Holger Caesar, Varun Bankiti, Alex H Lang, Sourabh Vora, Venice Erin Liong, Qiang Xu, Anush Krishnan, Yu Pan, Giancarlo Baldan, and Oscar Beijbom. nuscenes: A multi-modal dataset for autonomous driving. In *IEEE/CVF Conference on Computer Vision and Pattern Recognition (CVPR)*, pages 11621–11631, 2020. [2](#), [5](#), [6](#)
- [4] Nicolas Carion, Francisco Massa, Gabriel Synnaeve, Nicolas Usunier, Alexander Kirillov, and Sergey Zagoruyko. End-to-end object detection with transformers. In *European conference on computer vision (ECCV)*, pages 213–229. Springer, 2020. [1](#), [2](#), [3](#)
- [5] Qiang Chen, Xiaokang Chen, Jian Wang, Shan Zhang, Kun Yao, Haocheng Feng, Junyu Han, Errui Ding, Gang Zeng, and Jingdong Wang. Group detr: Fast detr training with group-wise one-to-many assignment. In *Proceedings of the IEEE/CVF International Conference on Computer Vision*, pages 6633–6642, 2023. [2](#)
- [6] Xiyang Dai, Yinpeng Chen, Jianwei Yang, Pengchuan Zhang, Lu Yuan, and Lei Zhang. Dynamic detr: End-to-end object detection with dynamic attention. In *IEEE/CVF International Conference on Computer Vision (ICCV)*, pages 2988–2997, 2021. [2](#)
- [7] Shuxiao Ding, Lukas Schneider, Marius Cordts, and Juergen Gall. Ada-track: End-to-end multi-camera 3d multi-object tracking with alternating detection and association. In *IEEE/CVF Conference on Computer Vision and Pattern Recognition (CVPR)*, pages 15184–15194, 2024. [1](#), [2](#), [3](#), [6](#), [7](#), [12](#), [13](#)
- [8] Simon Doll, Niklas Hanselmann, Lukas Schneider, Richard Schulz, Markus Enzweiler, and Hendrik PA Lensch. Star-track: Latent motion models for end-to-end 3d object tracking with adaptive spatio-temporal appearance representations. *IEEE Robotics and Automation Letters (RAL)*, 2023. [1](#), [3](#), [6](#)
- [9] Teng Fu, Xiaocong Wang, Haiyang Yu, Ke Niu, Bin Li, and Xiangyang Xue. Denoising-mot: Towards multiple object tracking with severe occlusions. In *Proceedings of the 31st ACM International Conference on Multimedia*, pages 2734–2743, 2023. [2](#), [3](#)
- [10] Yihan Hu, Jiazhi Yang, Li Chen, Keyu Li, Chonghao Sima, Xizhou Zhu, Siqi Chai, Senyao Du, Tianwei Lin, Wenhai Wang, et al. Planning-oriented autonomous driving. In *IEEE/CVF Conference on Computer Vision and Pattern Recognition (CVPR)*, pages 17853–17862, 2023. [1](#), [3](#)
- [11] Md Shamim Hussain, Mohammed J Zaki, and Dharmashankar Subramanian. Global self-attention as a replacement for graph convolution. In *28th ACM SIGKDD Conference on Knowledge Discovery and Data Mining*, pages 655–665, 2022. [3](#), [5](#), [6](#), [12](#)
- [12] Youngwan Lee, Joong-won Hwang, Sangrok Lee, Yuseok Bae, and Jongyoul Park. An energy and gpu-computation efficient backbone network for real-time object detection. In *IEEE/CVF Conference on Computer Vision and Pattern Recognition Workshops (CVPRW)*, 2019. [6](#)
- [13] Feng Li, Hao Zhang, Shilong Liu, Jian Guo, Lionel M Ni, and Lei Zhang. Dn-detr: Accelerate detr training by introducing query denoising. In *IEEE/CVF Conference on Computer Vision and Pattern Recognition (CVPR)*, pages 13619–13627, 2022. [2](#), [3](#), [4](#), [5](#)
- [14] Peixuan Li and Jieyu Jin. Time3d: End-to-end joint monocular 3d object detection and tracking for autonomous driving. In *IEEE/CVF Conference on Computer Vision and Pattern Recognition (CVPR)*, pages 3885–3894, 2022. [3](#)
- [15] Yanwei Li, Zhiding Yu, Jonah Philion, Anima Anandkumar, Sanja Fidler, Jiaya Jia, and Jose Alvarez. End-to-end 3d tracking with decoupled queries. In *IEEE/CVF International Conference on Computer Vision (ICCV)*, pages 18302–18311, 2023. [1](#), [3](#), [6](#)
- [16] Xuewu Lin, Tianwei Lin, Zixiang Pei, Lichao Huang, and Zhizhong Su. Sparse4d: Multi-view 3d object detection with sparse spatial-temporal fusion. *ArXiv*, abs/2211.10581, 2022. [2](#)
- [17] Xuewu Lin, Tianwei Lin, Zixiang Pei, Lichao Huang, and Zhizhong Su. Sparse4d v2: Recurrent temporal fusion with sparse model. *ArXiv*, abs/2305.14018, 2023.
- [18] Xuewu Lin, Zixiang Pei, Tianwei Lin, Lichao Huang, and Zhizhong Su. Sparse4d v3: Advancing end-to-end 3d detection and tracking. *ArXiv*, 2023. [2](#)
- [19] Shilong Liu, Feng Li, Hao Zhang, Xiao Yang, Xianbiao Qi, Hang Su, Jun Zhu, and Lei Zhang. Dab-detr: Dynamic an-

- chor boxes are better queries for detr. In *International Conference on Learning Representations (ICLR)*, 2022. 2
- [20] Yingfei Liu, Tiancai Wang, Xiangyu Zhang, and Jian Sun. Petr: Position embedding transformation for multi-view 3d object detection. In *European Conference on Computer Vision (ECCV)*, pages 531–548. Springer, 2022. 1, 2, 3
- [21] Tim Meinhardt, Alexander Kirillov, Laura Leal-Taixe, and Christoph Feichtenhofer. Trackformer: Multi-object tracking with transformers. In *IEEE/CVF Conference on Computer Vision and Pattern Recognition (CVPR)*, pages 8844–8854, 2022. 2, 12
- [22] Depu Meng, Xiaokang Chen, Zejia Fan, Gang Zeng, Houqiang Li, Yuhui Yuan, Lei Sun, and Jingdong Wang. Conditional detr for fast training convergence. In *IEEE/CVF International Conference on Computer Vision (ICCV)*, pages 3651–3660, 2021. 2
- [23] Ziqi Pang, Jie Li, Pavel Tokmakov, Dian Chen, Sergey Zagoruyko, and Yu-Xiong Wang. Standing between past and future: Spatio-temporal modeling for multi-camera 3d multi-object tracking. In *IEEE/CVF Conference on Computer Vision and Pattern Recognition (CVPR)*, pages 17928–17938, 2023. 1, 3, 6
- [24] Peize Sun, Jinkun Cao, Yi Jiang, Rufeng Zhang, Enze Xie, Zehuan Yuan, Changhu Wang, and Ping Luo. Transtrack: Multiple object tracking with transformer. *ArXiv*, abs/2012.15460, 2020. 3
- [25] Qitai Wang, Jiawei He, Yuntao Chen, and Zhaoxiang Zhang. Onetrack: Demystifying the conflict between detection and tracking in end-to-end 3d trackers. In *European Conference on Computer Vision (ECCV)*, pages 387–404. Springer, 2024. 3
- [26] Shihao Wang, Yingfei Liu, Tiancai Wang, Ying Li, and Xiangyu Zhang. Exploring object-centric temporal modeling for efficient multi-view 3d object detection. In *IEEE/CVF International Conference on Computer Vision (ICCV)*, pages 3621–3631, 2023. 2, 3
- [27] Shuo Wang, Fan Jia, Weixin Mao, Yingfei Liu, Yucheng Zhao, Zehui Chen, Tiancai Wang, Chi Zhang, Xiangyu Zhang, and Feng Zhao. Stream query denoising for vectorized hd-map construction. In *European Conference on Computer Vision (ECCV)*, pages 203–220. Springer, 2024. 3
- [28] Yue Wang, Vitor Campagnolo Guizilini, Tianyuan Zhang, Yilun Wang, Hang Zhao, and Justin Solomon. Detr3d: 3d object detection from multi-view images via 3d-to-2d queries. In *Conference on Robot Learning (CoRL)*, pages 180–191. PMLR, 2022. 1, 2
- [29] Xinhua Weng, Jianren Wang, David Held, and Kris Kitani. 3d multi-object tracking: A baseline and new evaluation metrics. In *IEEE/RSJ International Conference on Intelligent Robots and Systems (IROS)*, pages 10359–10366. IEEE, 2020. 6
- [30] Yihong Xu, Yutong Ban, Guillaume Delorme, Chuang Gan, Daniela Rus, and Xavier Alameda-Pineda. Transcenter: Transformers with dense representations for multiple-object tracking. *IEEE Transactions on Pattern Analysis and Machine Intelligence*, 45(6):7820–7835, 2022. 3
- [31] En Yu, Tiancai Wang, Zhuoling Li, Yuang Zhang, Xiangyu Zhang, and Wenbing Tao. Motrv3: Release-fetch supervision for end-to-end multi-object tracking. *arXiv preprint arXiv:2305.14298*, 2023. 3
- [32] Fangao Zeng, Bin Dong, Yuang Zhang, Tiancai Wang, Xiangyu Zhang, and Yichen Wei. Motr: End-to-end multiple-object tracking with transformer. In *European Conference on Computer Vision (ECCV)*, pages 659–675. Springer, 2022. 2, 12
- [33] Hao Zhang, Feng Li, Shilong Liu, Lei Zhang, Hang Su, Jun Zhu, Lionel Ni, and Heung-Yeung Shum. Dino: Detr with improved denoising anchor boxes for end-to-end object detection. In *International Conference on Learning Representations (ICLR)*, 2023. 2, 3, 4
- [34] Tianyuan Zhang, Xuanyao Chen, Yue Wang, Yilun Wang, and Hang Zhao. Mutr3d: A multi-camera tracking framework via 3d-to-2d queries. In *IEEE/CVF Conference on Computer Vision and Pattern Recognition Workshops (CVPRW)*, pages 4537–4546, 2022. 1, 2, 3, 6, 12
- [35] Yuang Zhang, Tiancai Wang, and Xiangyu Zhang. Motrv2: Bootstrapping end-to-end multi-object tracking by pre-trained object detectors. In *IEEE/CVF Conference on Computer Vision and Pattern Recognition (CVPR)*, pages 22056–22065, 2023. 3
- [36] Zelin Zhao, Ze Wu, Yueqing Zhuang, Boxun Li, and Jiaya Jia. Tracking objects as pixel-wise distributions. In *European Conference on Computer Vision (ECCV)*, pages 76–94. Springer, 2022. 3
- [37] Lijun Zhou, Tao Tang, Pengkun Hao, Zihang He, Kalok Ho, Shuo Gu, Wenbo Hou, Zhihui Hao, Haiyang Sun, Kun Zhan, et al. Ua-track: Uncertainty-aware end-to-end 3d multi-object tracking. *arXiv preprint arXiv:2406.02147*, 2024. 2, 3
- [38] Xizhou Zhu, Weijie Su, Lewei Lu, Bin Li, Xiaogang Wang, and Jifeng Dai. Deformable detr: Deformable transformers for end-to-end object detection. *arXiv preprint arXiv:2010.04159*, 2020. 2

TQD-Track: Temporal Query Denoising for 3D Multi-Object Tracking

Supplementary Material

| α^{FP} | α^{drop} | AMOTA \uparrow | AMOTP \downarrow | Recall \uparrow | MOTA \uparrow | IDS \downarrow |
|----------------------|------------------------|------------------|--------------------|-------------------|-----------------|------------------|
| 0 | 0 | 0.495 | 1.223 | 0.602 | 0.452 | 610 |
| 0.05 | 0 | 0.505 | 1.206 | 0.609 | 0.457 | 585 |
| 0.1 | 0 | 0.515 | 1.206 | 0.623 | 0.467 | 596 |
| 0.15 | 0 | 0.503 | 1.207 | 0.604 | 0.461 | 578 |
| 0.1 | 0.05 | 0.501 | 1.205 | 0.604 | 0.463 | 628 |
| 0.1 | 0.1 | 0.507 | 1.199 | 0.624 | 0.458 | 654 |

Table A. Ablation study on the ratio of adding false positives α^{FP} and the ratio of randomly drop denoising samples α^{drop} .

| λ | σ_{velo} | σ_{query} | AMOTA \uparrow | AMOTP \downarrow | Recall \uparrow | MOTA \uparrow | IDS \downarrow |
|-----------|------------------------|-------------------------|------------------|--------------------|-------------------|-----------------|------------------|
| 0.8 | 4 | 0.1 | 0.502 | 1.207 | 0.616 | 0.462 | 595 |
| 1.2 | 4 | 0.1 | 0.505 | 1.202 | 0.597 | 0.455 | 525 |
| 1 | 2 | 0.1 | 0.506 | 1.203 | 0.595 | 0.459 | 587 |
| 1 | 6 | 0.1 | 0.495 | 1.21 | 0.602 | 0.445 | 583 |
| 1 | 4 | 0.05 | 0.495 | 1.207 | 0.603 | 0.453 | 590 |
| 1 | 4 | 0.2 | 0.499 | 1.202 | 0.586 | 0.45 | 603 |
| 1 | 4 | 0.1 | 0.515 | 1.206 | 0.623 | 0.467 | 596 |

Table B. Ablation study on the noise scales. λ is the scale of center shiftings, σ_{velo} is the variance of the velocity noises, and σ_{query} is the scale of feature query noises.

| N_{D} | AMOTA \uparrow | AMOTP \downarrow | Recall \uparrow | MOTA \uparrow | IDS \downarrow |
|----------------|------------------|--------------------|-------------------|-----------------|------------------|
| 300 | 0.499 | 1.215 | 0.602 | 0.457 | 725 |
| 400 | 0.496 | 1.197 | 0.612 | 0.451 | 648 |
| 500 | 0.515 | 1.206 | 0.623 | 0.467 | 596 |

Table C. Ablation study on the number of detection queries N_{D} initialized at each frame.

A. Additional Ablation Studies

Instance-level Noise As described in Eq. 5, we add the Top- k false positives from the detection queries to the denoising query set as negative denoising samples and they will be matched with the background at the next frame. In our method, k is dynamically determined by a hyperparameter α^{FP} , i.e. $k = \alpha^{\text{FP}} N_{\text{GT}}^t$, where N_{GT}^t denotes the number of ground truth objects at frame t . As a complementary study, we can also randomly drop denoising queries using a drop ratio α^{Drop} which represents the possibility that each positive denoising query is dropped. Note that the sampling of random add and random drop are independent in each denoising group. Table A shows the evaluation on α^{FP} and α^{drop} . When the drop ratio α^{drop} is set to 0, in-

creasing the false positive ratio α^{FP} improves the tracker’s performance up to an optimal value of $\alpha^{\text{FP}} = 0.1$. When further increasing α^{FP} to 0.15, the tracking performance decreases compared to $\alpha^{\text{FP}} = 0.1$, indicating that adding too many false positives could lead to data imbalance. We then set false positive ratio α^{FP} to 0.1 and evaluate α^{drop} . As shown in the bottom part Table A, increasing the drop ratio α^{drop} results in a decrease in the tracker’s performance compared to $\alpha^{\text{drop}} = 0$. This is because randomly dropping denoising queries reduces the number of denoising training samples available for the tracker to learn from. Based on this ablation study, we set $\alpha^{\text{FP}} = 0.1$ and disable random drop in our experiments.

Noise Scales Tuning Three types of noises are added to the denoising queries, including uniform noise for the 3D center as Eq. 2, Gaussian noise for the BEV velocity as Eq. 4, and Gaussian noise for the query feature as Eq. 3. Each type of noise has a corresponding noise scale which controls the noise intensity. For the uniform noise added to the center, the scale is controlled by λ ; for the Gaussian noise added to the BEV velocity and the query feature, the scale is controlled by σ_{velo} and σ_{query} , respectively. We set $\Sigma^{\text{velo}} = \sigma_{\text{velo}} \mathbf{I} \in \mathbb{R}^{2 \times 2}$ and $\Sigma^{\text{query}} = \sigma_{\text{query}} \mathbf{I} \in \mathbb{R}^{d_k \times d_k}$, where d_k is the feature dimension and \mathbf{I} is the identity matrix. The larger the noise scale, the more noisy the denoising queries will be. Table B shows the ablation study on the above mentioned noise scales. Empirically we set $\lambda = 1$, $\sigma_{\text{velo}} = 4$ and $\sigma_{\text{query}} = 0.1$ in our experiments due to their best performance in the ablation study.

Number of Det. Queries The number of detection queries N_{D} also affects the tracker’s performance. We conduct an ablation study on the number of detection queries on our TQD-Track and the results are shown in table C. The tracker achieves the best performance in terms of AMOTA when $N_{\text{D}} = 500$, and the Recall metric is consistently improved as the number of detection queries increases. It’s worth noting that our TQD-Track with 300 detection queries (49.9% AMOTA) already outperforms the ADA-Track baseline with 500 detection queries (49.3% AMOTA), which indicates the superiority of our proposed temporal query denoising method.

Scalability to Training Data Volume We evaluate the scalability of TQD-Track to the training data volume by varying the amount of nuScenes training set. In Figure A, we compare AMOTA of TQD-Track with ADA-Track with

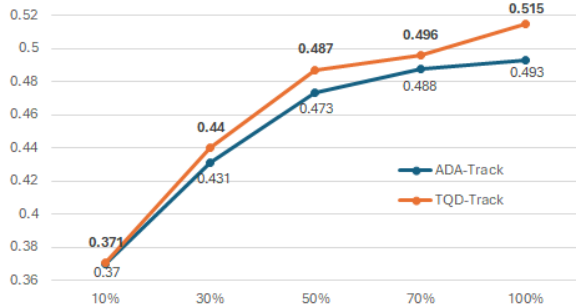


Figure A. **AMOTA vs. Portion of nuScenes training data** by scaling the nuScenes training set.

respects to the portions of the training set. We start with only 10% training set and both baseline and our TQD-Track achieve similar 37% AMOTA. By increasing the portions, TQD-Track consistently outperforms the baseline track across all the portion settings, and the performance gap between both methods tends to larger. This could be attribute to the ability in augmenting diverse training samples of query denoising in TQD-Track, where more training data could lead to exponentially increased data diversity. Notably, our TQD-Track achieves 49.6% AMOTA when only using 70% training set, which is better than the baseline tracker trained on the full training set (49.3% AMOTA), showing its potential with limited training data.

B. Model Details

We intergrated our temporal denoising method in multiple tracking paradigms, including tracking-by-attention (TBA), tracking-by-detection (TBD) and alternating detection and association (ADA). While tracking-by-attention (TBA) is a well-established and standard DETR-based tracker, see [21, 32, 34], ADA is introduced in a more recent work [7]. Therefore we explain some details of ADA as well as the TBD-Baseline from ADA-Track, which we also used as baseline in this work. We also refer to ADA-Track [7] for more details.

B.1. Details of ADA-Track

ADA-Track [7] is a state-of-the-art multi-camera 3D MOT method which introduces the Alternating Detection and Association paradigm to overcome the weaknesses of both tracking-by-attention and tracking-by-detection paradigms. At frame t , the multi-view images I_c^t captured from surrounding c cameras are first processed by a CNN image backbone to extract the feature maps F_c^t . The input queries to the transformer decoder consist of two parts, namely the track queries Q_T^t propagated from the previous frame and the detection queries Q_D^t randomly initialized. In ADA-

Track, the track queries Q_T^t are tasked to consistently detect the corresponding tracked objects, while the detection queries Q_D^t are designed to detect all objects in the current frame t . To encode the positional information of the queries, each query is assigned with a 3D reference point. The reference points C_T^t for track queries Q_T^t are derived from the centers of the track boxes \hat{B}_T^{t-1} from the previous frame $t-1$ after a motion update, while the reference points C_D^t for detection queries Q_D^t are initialized by uniformly sampling in the tracking space. These two sets of queries as well as the edge features $E \in \mathbb{R}^{(N_D N_T) \times d_k}$ which are encoded from box differences between each track-detection query pair are also fed into the model with L_d transformer decoder layers. Each decoder layer applies a self-attention between queries before a cross-attention between queries and image features F_c^t . Then, an Edge-Augmented Cross-Attention [11] module takes both query sets and the edges features as inputs to learn the data association between track and detection queries.

Formally (we omit the timestamp t for simplicity here), the attention score of the Edge-Augmented Cross-Attention can be calculated as

$$A = \frac{(Q_D W_Q)(Q_T W_K)^T}{\sqrt{d_k}} + E W_{E1}, \quad (\text{A})$$

where $\{W_Q, W_K\} \in \mathbb{R}^{d_k \times d_k}$ and $W_{E1} \in \mathbb{R}^{d_k}$ are learnable weights. The attention $A^{(l)} = \{a_{ij}^{(l)}\}$ will be normalized among the second dimension j using a softmax function, *i.e.*

$$\hat{a}_{ij} = \text{softmax}(a_{ij})_j = \frac{\exp(a_{ij})}{\sum_k \exp(a_{ik})}. \quad (\text{B})$$

The resulting normalized attention $\hat{A} = \{\hat{a}_{ij}\}$ is used to update the detection query features by

$$Q_D \leftarrow Q_D + \hat{A}(Q_T W_V), \quad Q_D \leftarrow Q_D + \text{FFN}_D(Q_D). \quad (\text{C})$$

In contrast, edge features are updated using A , *i.e.*

$$E \leftarrow E + A W_{E2}, \quad E \leftarrow E + \text{FFN}_E(E), \quad (\text{D})$$

where $W_V \in \mathbb{R}^{d_k \times d_k}$ and $W_{E2} \in \mathbb{R}^{d_k}$ denote learnable weights, FFN_D and FFN_E denote Feed-Forward-Networks (FFN). We omit the Layer Normalization [1] in Eq. C and Eq. D for simplicity.

In this way, the detection and association tasks are alternatively conducted across the L_d decoder layers, forming the Alternating Detection and Association (ADA) paradigm. At the end of the decoder, MLP-based task heads predict the bounding boxes B_T^t and B_D^t from the refined track queries Q_T^t and detection queries Q_D^t , respectively. Another MLP predict the association score S between tracks and detections based on the final edge features E^t . Finally, a track update module takes B_T^t and B_D^t along

with their respective refined queries Q_T^t and Q_D^t as well as the association score S as inputs, conducts an Hungarian Matching using S , and outputs the updated track queries \hat{Q}_T^t and track boxes \hat{B}_T^t based on the matching results.

B.2. Details of TBD-Baseline

Tracking-by-Detection is a traditional tracking paradigm that first detect objects and then associate the detected objects with the tracks in the memory. We follow the implementation of TBD-Baseline in ADA-Track [7]. Concretely, the model consists of a detector and a data association decoder. Track Q_T^t and detection queries Q_D^t with their reference points C_T^t , C_D^t are fed into the detector. The detector consists of transformer decoder layers with a self-attention between queries and a cross-attention between queries and image features, producing track and detection bounding boxes B_T^t and B_D^t . The decoder layer is same as in the ADA-Track, *i.e.* Eq. A, Eq. B, Eq. C and Eq. D. However, they are not integrated into detector’s decoder layer as in ADA-Track but are stacked in the association decoder, corresponding to the modular design of tracking-by-detection. The track update module remains the same as in ADA-Track.